Hindawi Publishing Corporation
Shock and Vibration
Volume 2016, Article ID 7383679, 11 pages
http://dx.doi.org/10.1155/2016/7383679

Research Article

High Response Performance of a Tuned-Mass Damper for Vibration Suppression of Offshore Platform under Earthquake Loads

Qiong Wu,[1] Xilu Zhao,[1] Rencheng Zheng,[2] and Keisuke Minagawa[1]

[1]*College of Mechanical Engineering, Saitama Institute of Technology, Saitama 369-0293, Japan*
[2]*Institute of Industrial Science, The University of Tokyo, Tokyo 153-8505, Japan*

Correspondence should be addressed to Qiong Wu; wuqiong55@126.com

Received 14 November 2015; Revised 19 March 2016; Accepted 24 March 2016

Academic Editor: Salvatore Strano

Currently, tuned-mass dampers (TMDs) are widely applied to maintain the stability of offshore platforms in hostile environments; however, the stability system of offshore platforms faces considerable challenges under critical earthquake loads of the initial period. Therefore, this study concentrated on the high response performance of a simple passive TMD system, and numerical and experimental investigations were performed using a 1 : 200-scale prototype. The obtained results indicated that the displacement, acceleration, and their power spectral density all decreased significantly for the offshore platform with the TMD system. By further analyses of its high response characteristics, it was validated that the TMD reactions can commence within the first 3 s of earthquake excitation, while the fundamental natural frequency was consistently tuned for the TMD system dependent on the dynamic magnification factor. The evaluation indices also confirmed that this method is effective in reducing the overall vibration level and the maximum peak values of the offshore platform exposed to earthquake excitations, mainly because of its high response characteristics.

1. Introduction

Offshore platforms of the offshore oil industry are used for exploration drilling, tender-assisted drilling, production, accommodation, and maintenance [1]. Such offshore structures, which can be located in hostile environments, are always exposed to loadings from wind, waves, and sometimes earthquakes, the latter being one of the most violent loadings these structures might endure. Therefore, it is necessary to study the relationship between irregular loadings and the corresponding response of offshore structures to derive effective vibration-suppression systems or techniques [2].

In deep-water environments, offshore platforms are susceptible to vibration induced by the action of waves, which not only affects their structural strength but also has considerable impact on their reliability and safety [3]. Accident rates due to the effects of vibration and structural deficiencies remain comparatively high, making an accurate analysis of jack-up behaviors increasingly important. Recent attention has focused on understanding the behaviors of offshore platforms under dynamic loading conditions [4]. Jack-up platforms are flexible structures built to have natural periods of the same order as the predominant wave periods for many seas, which are designed based on structural modeling of the legs, analysis of the degree of flexibility provided by the spudcan, and assessment of the nature of the wave loads [5]. These sophisticated structures generally result in self-excited nonlinear hydrodynamic forces, and the resulting large deformations, in turn, cause a highly nonlinear response [6].

In recent decades, vibration-control technologies, implemented based on platform type, have achieved significant success in mitigating the vibration of land-based structures [7]. For example, a network-based modeling and active tuned-mass damper mechanism was investigated for an offshore steel jacket platform, which can be significantly capable of reducing the required control force and the oscillation amplitudes of the offshore platform [8]. Moreover, a typical tension-leg type of floating platform had been studied, which incorporated a tuned-liquid-column damper [9]. Recently, Zhang et al. [10] developed a sliding mode H_∞ control to

improve the control performance of the offshore platform, subject to wave-induced force as well as external disturbance. In addition, compared with the H_∞ control scheme, a network-based modeling and event-triggered H_∞ reliable control for an offshore structure was proposed [11]. It can suppress the vibration of the offshore structure to almost the same level as the H_1 controller, while the former requires less control cost. Specifically, a more general uncertain dynamic model of the offshore platform was developed, and then a novel delayed sliding mode control scheme using mixed current and delayed states was proposed in [12]. It is shown through the simulating results that this scheme is more effective in both improving the control performance and reducing control force of the offshore platform.

Gattulli and Ghanem [13] developed an active mass damper control technique for the suppression of vortex-induced vibrations in offshore structures, and Kawano [14] investigated semiactive control devices applied in jack-up offshore platforms, in which the active control force is determined using a time-domain transient optimal control method. Zhou et al. [15] proposed a semiactive control method utilizing the energy-dissipation principle and a bang-bang control based on a linear quadratic regulator optimal control theory. Amongst the various semiactive control devices, a magnetorheological damper has been studied for structural vibration control, and the simulated results indicated that such a system could provide quick reaction with little time delay, insensitivity to temperature, and small power requirement [16].

However, offshore platforms are located in ocean environments, which could increase the cost of maintenance of active and semiactive systems and indirectly increase the risk to staff. Therefore, passive vibration control might be the most suitable and feasible strategy for vibration control in offshore platforms.

A passive TMD was studied for the reduction of vibration in flexible structures subjected to long-reduction narrow excitations [17]. This was conducted because, amongst the numerous passive control techniques, the TMD is one of the simplest control devices [18]. The determination of the optimal parameters has been performed according to the different objectives of reducing the maximum displacements, story drifts, and base shear, for different harmonic, white noise, and earthquake excitations [19]. Li and Zhu [20] proposed using double TMDs, in which the mass damper was optimized for high effectiveness and robustness in reducing undesirable vibrations under the effects of ground acceleration. Bekdaş and Nigdeli [21] found a mathematical optimization method using harmony search, which was applied successfully to passive TMDs. Yu et al. [22] outlined a robust design optimization framework dedicated to TMDs.

Many researchers have studied the applicability of TMDs to ground-based structures subject to seismic excitation [23–25]. For an earthquake excitation in which its duration is substantially shorter, considerable disasters often occurred during the initial period of an earthquake load. The several previous studies used the tuned-mass damper with viscous damping to improve the vibration-control effectiveness. However, because the high response performance of tuned-mass damper is not considered, these dampers may not have enough reaction time to produce a significant effect in the initial seconds of the earthquake excitation. Tsai [26] simulated TMDs with different parameters under different earthquake excitations. It was found that a TMD with damping had little reaction to the structural response in the initial seconds following the occurrence of an earthquake; therefore, a virtual accelerator was proposed to improve the TMD performance. Lin et al. [27] studied an undamped TMD with a resettable variable stiffness device, which could avoid detuning effects and assure optimal control performance. Zhang and Balendra [28] investigated the feasibility of adopting a TMD for the control of an inelastic structure subject to seismic motions. Marano et al. [29] dealt with the optimal design of a TMD to reduce undesirable vibrational effects, which were originated in linear structures by seismic excitations. However, based on our literature review, passive TMD technology has had little application to the control of the response of offshore platforms to an earthquake because of the complexity of the excitation. Many control strategies have been shown effective in the mitigation of structural vibration; however, few studies have examined the response performance of a TMD at the onset of earthquake excitation. In order to reduce the risk of damage to jack-up offshore platforms in harsh marine environments, studies are required to develop efficient and practical vibration-control strategies that can suppress the dynamic response of offshore structures.

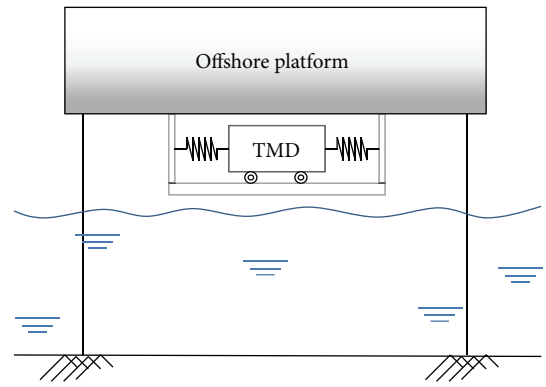

Figure 1: Schematic of a jack-up offshore platform with a tuned-mass damper (TMD).

This study involved comprehensive experimental and analytical investigations to extend the understanding of the high response performance of TMD systems under two seismic stimuli. The experimental process was based on a prototype in an experimental setting. In the following sections, the results of the amplitude and frequency responses, relative motion, high response characteristics, and evaluation indices are interpreted. In addition, the tuned-mass damper control scheme will be compared with some existing control schemes, such as tuned-liquid damper [30] and active mass damper control scheme [31].

2. Methods and Materials

2.1. Modeling. To analyze the effectiveness of a TMD, an actual jack-up offshore platform (Bohai number 5, located in the Southern Sea) [32] was considered as the research target. As demonstrated in Figure 1, the jack-up offshore platform

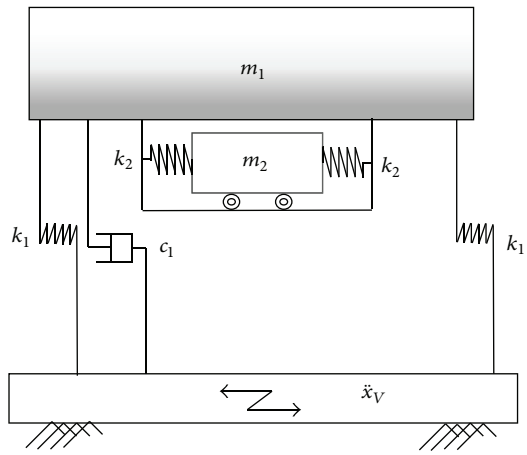

Figure 2: Systemic modeling of a jack-up offshore platform with a tuned-mass damper (TMD).

comprises a rectangular platform resting on four independent operating legs, with a TMD attached beneath the platform. The TMD device consists of a frame, a mass, two springs, four wheels, and two tracks. The size of the working platform is $57.5 \times 34.0 \times 5.50$ m, the length and diameter of the operating legs are 78 and 3 m, respectively, and the limit of the operating water depth is 40 m.

As presented in Figure 2, a systemic model of a jack-up offshore platform with a TMD can be considered as a general structure ($m_1 + m_2$) that includes the main structure of the offshore platform (m_1) and the substructure of the TMD (m_2). Thereby, the dynamic model can be expressed as

$$\begin{aligned} m_1\ddot{x}_1 + c_1\dot{x}_1 + k_1x_1 - k_2\left(x_2 - x_1\right) &= -m_1\ddot{x}_V, \\ m_2\ddot{x}_2 + k_2\left(x_2 - x_1\right) &= -m_2\ddot{x}_V, \end{aligned} \tag{1}$$

where m_1, c_1, and k_1 are the mass, damping, and stiffness of the main structure, respectively; m_2 and k_2 are the mass and stiffness of the substructure, respectively; and $\ddot{x}_V$ is the acceleration vector of the seismic loads.

To resolve (1), while $x_1 = X_1e^{iwt}$ and $x_2 = X_2e^{iwt}$ [33], the imaginary amplitudes of the main structure X_1 and substructure X_2 can be expressed as

$$X_1 = \left|X_1e^{iwt}\right| = \frac{m_1\ddot{x}_V\left(k_2 - m_2w^2\right)}{\sqrt{{c_1}^2w^2\left(k_2 - m_2w^2\right)^2 + \left[\left(k_1 + k_2 - m_1w^2\right)\left(k_2 - m_2w^2\right) - {k_2}^2\right]^2}}, \tag{2}$$

$$X_2 = \left|X_2e^{iwt}\right| = \frac{m_2\ddot{x}_Vk_2}{\sqrt{{c_1}^2w^2\left(k_2 - m_2w^2\right)^2 + \left[\left(k_1 + k_2 - m_1w^2\right)\left(k_2 - m_2w^2\right) - {k_2}^2\right]^2}}, \tag{3}$$

where w is the excitation frequency of the seismic loads.

From (2), the dynamic magnification factor for the main structure can be described as

$$\left|\frac{X_1}{X_{\mathrm{st}}}\right| = \sqrt{\frac{\left(\eta^2 - \lambda^2\right)^2}{\left[\left(\eta^2 - \lambda^2\right)\left(1 - \lambda^2\right) - \mu\eta^2\lambda^2\right]^2 + \left[2\xi_1\lambda\left(\eta^2 - \lambda^2\right)\right]^2}}, \tag{4}$$

where $X_{\mathrm{st}} = m_1\ddot{x}_V/k_1$ is the static displacement of the main structure, $\eta = w_2/w_1$ is the natural frequency ratio, $w_1 = \sqrt{k_1/m_1}$ and $w_2 = \sqrt{k_2/m_2}$ are the natural frequencies of the main structure and substructure, respectively, $\lambda = w/w_1$ is the ratio of the excitation and natural frequencies of the main structure, and $\xi_1 = c_1/2m_1w_1$ is the damping ratio of the main structure.

Based on (4), the dynamic magnification factor becomes zero, while $\eta = \lambda$, which indicates that optimal vibration reduction will be achieved when exposed to the specific excitation frequencies of the seismic loads. The seismic loads involve different frequency components, which can result in the maximum amplitude vibration of the main structure during the range of the resonance frequency. Therefore, when the natural frequency of the TMD is adjusted to the natural frequency of the structure, the TMD will be in a resonant state. Therefore, a large amount of the structural vibration energy will be transferred to the TMD, and, thus, vibration reduction can be achieved. By modeling the offshore platform with a fixed TMD, the natural frequency can be measured during experimental testing.

2.2. Numerical Analysis. By application of the central difference method to solve (1) [34] using time step i, the differential acceleration and velocity can be expressed as

$$\begin{aligned} \ddot{x}^{(i)} &= \frac{x^{(i+1)} - 2x^{(i)} + x^{(i-1)}}{\Delta^2t}, \\ \dot{x}^{(i)} &= \frac{x^{(i+1)} - x^{(i-1)}}{2\Delta t}, \end{aligned} \tag{5}$$

where Δt is the time increment. When (5) are substituted into (1), the formula for the calculation of the displacement difference can be expressed as

$$x_1^{(i+1)} = \frac{\left(2m_1 - k_1\Delta^2 t - k_2\Delta^2 t\right) x_1^{(i)} + k_2\Delta^2 t x_2^{(i)} + \left(-m_1 + 0.5c_1\Delta t\right) x_1^{(i-1)} - m_1\ddot{x}_V\Delta^2 t}{m_1 + 0.5c_1\Delta t},$$
$$x_2^{(i+1)} = \frac{\left(2m_2 - k_2\Delta^2 t\right) x_2^{(i)} + k_2\Delta^2 t x_1^{(i)} - m_2 x_2^{(i-1)} - m_2\ddot{x}_V\Delta^2 t}{m_2}. \quad (6)$$

The initial conditions of the offshore platform can be expressed as

$$\begin{aligned} x_1^{(0)} &= 0, \\ \dot{x}_1^{(0)} &= 0, \\ \ddot{x}_1^{(0)} &= 0, \\ x_2^{(0)} &= 0, \\ \dot{x}_2^{(0)} &= 0, \\ \ddot{x}_2^{(0)} &= 0. \end{aligned} \quad (7)$$

When the initial conditions of (7) are substituted into (5), the two initial displacements will be zero; for example,

$$\begin{aligned} x_1^{(1)} &= 0, \\ x_2^{(1)} &= 0. \end{aligned} \quad (8)$$

Inserting the initial displacements of the second step $x_1^{(0)} = 0$, $x_2^{(0)} = 0$, $x_1^{(1)} = 0$, and $x_2^{(1)} = 0$ into (6) means that the subsequent differential displacements $x_1^{(2)}$ and $x_2^{(2)}$ can be obtained. By continually increasing the calculation step, the differential displacements of $x_1^{(i+1)}$ and $x_2^{(i+1)}$ can be estimated from $x_1^{(i-1)}$, $x_2^{(i-1)}$, $x_1^{(i)}$, and $x_2^{(i)}$.

2.3. Evaluation Index. A root mean square (RMS) of the displacement or acceleration response can be expressed as

$$\mathrm{RMS} = \sqrt{\frac{1}{n}\sum_{i=1}^{n} y_i^2}, \quad (9)$$

where y_i is the sampling value of the displacement or acceleration response.

To evaluate effectiveness of the vibration reduction during the entire earthquake period, an evaluation index was proposed:

$$J = \frac{\mathrm{RMS}_{\mathrm{ctrl}}}{\mathrm{RMS}_{\mathrm{unctrl}}}, \quad (10)$$

where $\mathrm{RMS}_{\mathrm{ctrl}}$ and $\mathrm{RMS}_{\mathrm{unctrl}}$ are the RMS values of the displacement or acceleration responses of the main structure for the entire earthquake period, for the cases with and without the TMD system, respectively.

To evaluate the maximum response reduction, a maximum peak value was selected as $y_{\max} = \max\{y_i\}$. Then, a relative ratio of the maximum peak values can be obtained from

$$\beta = \frac{y_{\text{max-unctrl}} - y_{\text{max-ctrl}}}{y_{\text{max-unctrl}}}, \quad (11)$$

where $y_{\text{max-ctrl}}$ and $y_{\text{max-unctrl}}$ are the maximum peak values of the displacement or acceleration responses of the main structure with and without the TMD system, respectively.

3. Experiment

3.1. Apparatus. As shown in Figure 3, the testing system comprised a personal computer, vibration signal generator, amplifier, shaker, offshore platform system, acceleration sensor, laser displacement sensor, and fast Fourier transform analyzer. In the experiment, the sand height was 80 mm and the water depth was 400 mm. The mass of the offshore platform as the main structure (m_1) was 2.346 kg and the mass of the TMD was 0.591 kg. Through experimental validation, the damping coefficient was determined as 0.012.

As shown in Figure 4, a 1 : 200-scale four-column type of offshore platform was constructed. The operating platform was simplified to a horizontal rectangular metal mass. The supporting columns were simplified to hollow tubes. Cylindrical pile shoes were set at the roots of the columns and the connections between the columns and the operating platform were rigid. The offshore platform was placed in a tank that was fixed on the shaker, which simulated the seismic loads.

3.2. Process. Initially, the substructure of the TMD was installed at the bottom of the offshore platform to measure the first natural frequency of the complete structure. The input signal was a 0–8 Hz sweep signal.

The second step was to remove the substructure from the offshore platform and to attach it to the shaker. Then, the spring stiffness of the TMD was adjusted to make the first natural frequency of the substructure the same as that of the main structure. As shown in Figure 5, the peak frequency response function of both was 2.56 Hz.

In the third step, two types of seismic wave (El-Centro NS and Taft EW) [35] were generated by the signal generator and fed to the shaker to evaluate the effectiveness of the vibration-control system. The recording time was 25 s and the sampling frequency was 50 Hz for the two seismic waves. Consequently, the displacement and acceleration of the main structure and the relative displacement between the main structure and the substructure were recorded.

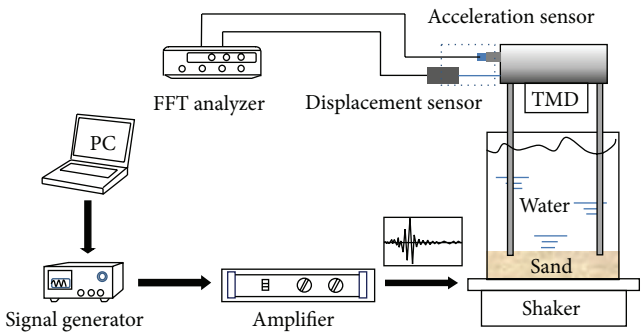

Figure 3: Diagram of testing system (PC: personal computer, TMD: tuned-mass damper, and FFT analyzer: fast Fourier transform analyzer).

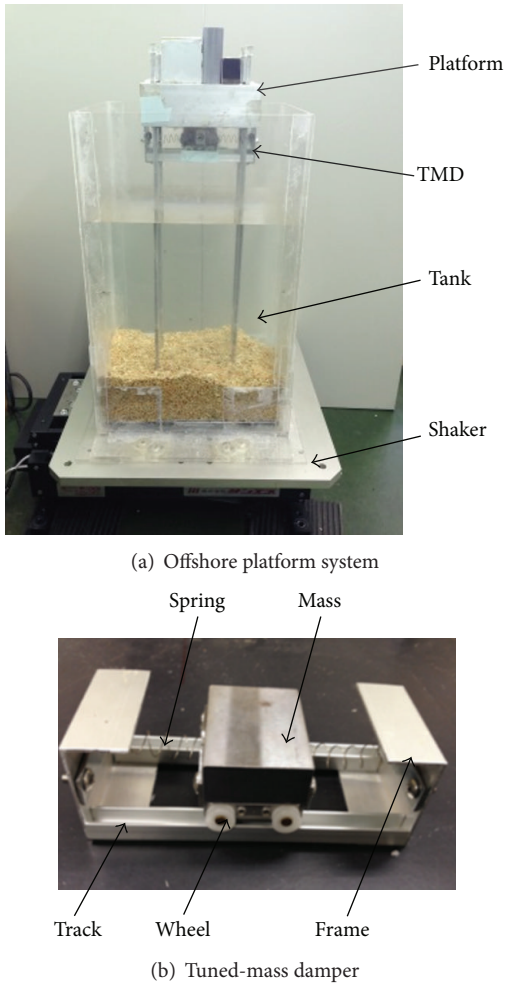

(a) Offshore platform system

(b) Tuned-mass damper

Figure 4: Experimental setting: (a) offshore platform and (b) tuned-mass damper (TMD).

Here, the El-Centro NS was the NS component recorded at the Imperial Valley Irrigation District substation in El Centro, California, USA, on May 18, 1940. Its magnitude was 6.9 and the peak acceleration was 341 cm/s^2. The Taft EW was the EW component recorded at Kern County, California, USA, on July 21, 1952. Its magnitude was 7.7 and the peak acceleration value was 175.9 cm/s^2 [36].

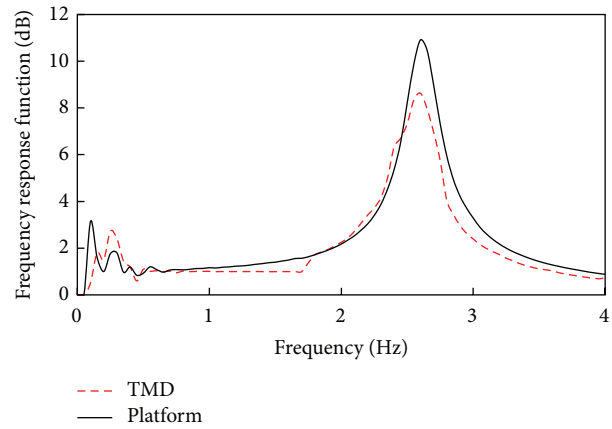

Figure 5: Frequency response analysis of the tuned-mass damper (TMD) and offshore platform.

4. Results

4.1. Amplitude Response Analysis. Figures 6 and 7 display the time series of the responses of the main structure with and without the TMD under the excitation of the El-Centro NS and Taft EW seismic waves. The experimental results of the displacement response are shown in Figures 6(a) and 6(c) and the numerical values of the displacement response are shown in Figures 6(b) and 6(d). The experimental results of the acceleration response are shown in Figure 7.

The numerical analyses show that the peak values of the displacement responses decreased significantly with TMD control compared with those cases without TMD control. It can be seen that this decreasing tendency was more significant for the acceleration responses. The results of the experimental analyses are consistent with the numerical analyses, and the accuracy of the numerical method is verified by the similarity between the amplitudes obtained from the simulation and the experiment. However, the numbers of wave peaks obtained in the numerical analyses are greater than in the experimental analyses because of the ideal conditional setting of the numerical method. These results indicate that the control performance of the TMD is as effective as an energy-dissipation device for the reduction of the main structural response.

It is particularly important for vibration suppression under excitation by seismic waves that the TMD can effectively reduce the relatively high-amplitude displacements and accelerations. These high-amplitude displacements occurred during the early period of the test and the TMD responded quickly to these early vibration excitations. For the relatively low-amplitude displacements and accelerations, the TMD control resulted in little effective reduction; however, these low-amplitude locals provided only a small contribution to the platform vibration.

4.2. Frequency Response Analysis. Based on a frequency response analysis, the power spectral density (PSD) of the displacement of the main structure is presented in Figure 8 and the PSD of the acceleration of the main structure is

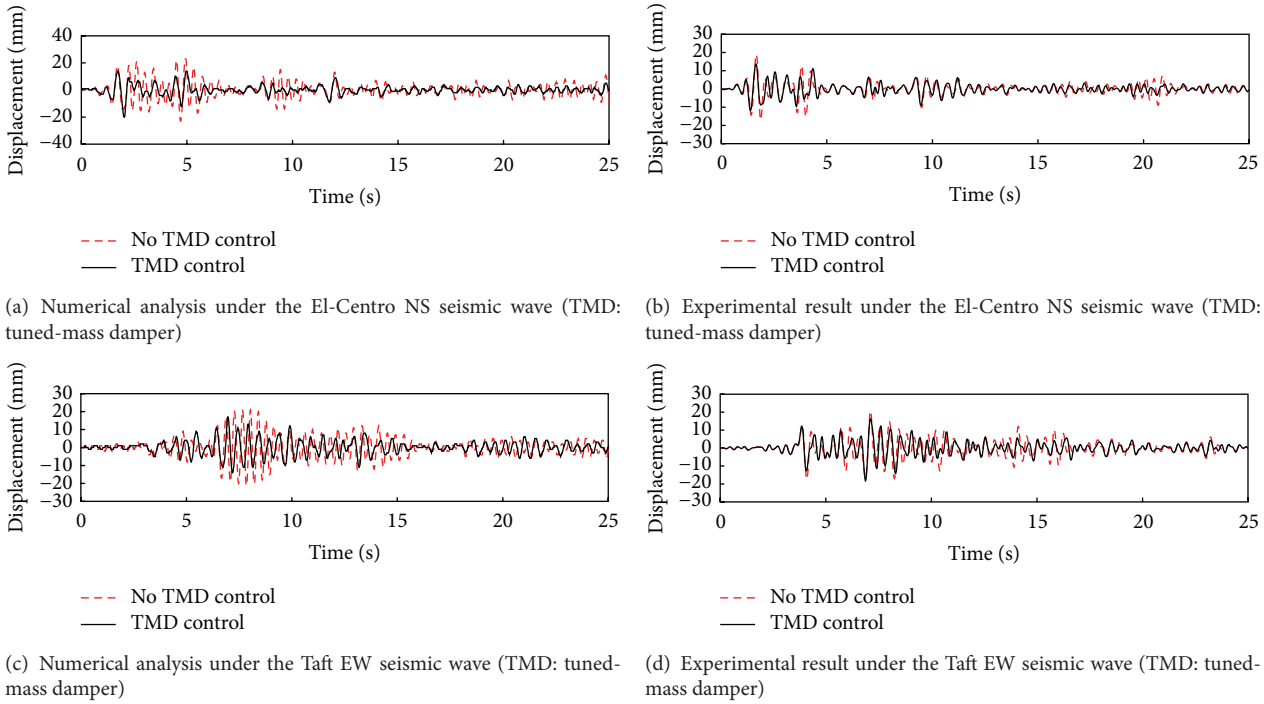

(a) Numerical analysis under the El-Centro NS seismic wave (TMD: tuned-mass damper)

(b) Experimental result under the El-Centro NS seismic wave (TMD: tuned-mass damper)

(c) Numerical analysis under the Taft EW seismic wave (TMD: tuned-mass damper)

(d) Experimental result under the Taft EW seismic wave (TMD: tuned-mass damper)

Figure 6: Displacement responses under the El-Centro NS and Taft EW seismic waves: (a) numerical analysis under the El-Centro NS, (b) experimental result under the El-Centro NS, (c) numerical analysis under the Taft EW, and (d) experimental result under the Taft EW.

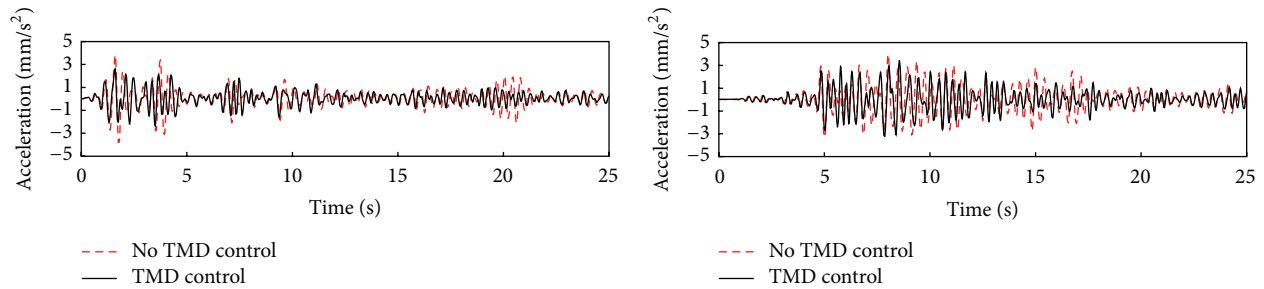

(a) Experimental result under the El-Centro NS seismic wave (TMD: tuned-mass damper)

(b) Experimental result under the Taft EW seismic wave (TMD: tuned-mass damper)

Figure 7: Experimental results of the acceleration responses under (a) the El-Centro NS and (b) the Taft EW seismic waves.

presented in Figure 9. It is obvious that the high amplitude of the PSD is around 2.56 Hz for the case without TMD control, because the resonance reaction of the main structure occurred around this frequency domain; this can explain why the designed TMD frequency was nearly 2.56 Hz, as mentioned in relation to Figure 5. Therefore, in the case with TMD control, it is significantly effective in reducing the vibration response of the main structure; in particular, the peak responses are reduced considerably around the 2.56 Hz frequency domain.

It is validated that the overall vibration response can be decreased significantly by reducing the first-mode vibration, and these results of the PSD curves explain why the time series response is effective in vibration reduction. Consequently, a single damper tuned to the fundamental mode is adequate for reducing the structural vibration under earthquake excitations. Investigation of frequency regions other than the fundamental frequency revealed no negative effects in the nondominant frequency regions.

4.3. Evaluation Index. The control performance was analyzed by application of the indices of β and J, which are defined in (10) and (11), respectively. The β index is the ratio of the RMS values of the displacements or accelerations of the offshore platform between the cases with and without the TMD control. The J index is the relative ratio of the peak values between the cases with and without the TMD control.

As shown in Table 1, the J values for the displacement response are >0.80, which indicates that the vibration of

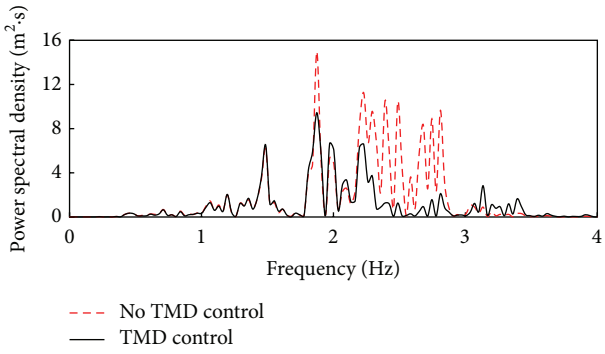

(a) Power spectral density under the El-Centro NS seismic wave (TMD: tuned-mass damper)

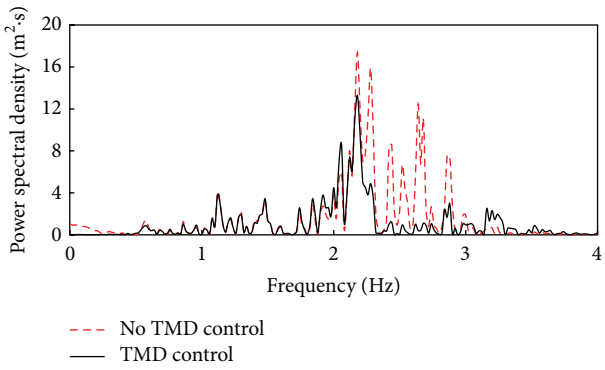

(b) Power spectral density of the Taft EW seismic wave (TMD: tuned-mass damper)

Figure 8: Power spectral density of the displacement under (a) the El-Centro NS and (b) the Taft EW seismic waves.

Table 1: Results of the evaluation indices.

Seismic excitation	Displacement response		Acceleration response	
	J	β	J	β
El-Centro NS	0.8049	0.2805	0.7722	0.3239
Taft EW	0.8191	0.2744	0.7283	0.4406

the platform was improved significantly during the entire earthquake period when the TMD was used. Moreover, analysis of the β values shows that a reduction of >27% was accomplished for the peak displacement response by the application of the TMD system.

For the acceleration displacement response, the J values are >0.70, which means that the dynamic performance was also improved considerably throughout the entire earthquake period. Similarly, the β values are >0.30, which means the peak response was decreased by 30% by the application of the TMD system.

5. Discussion

It can be seen from the above experimental results that the TMD system can effectively suppress the seismic motion for an offshore platform model. In order to further the understanding of the dynamic performances of the TMD,

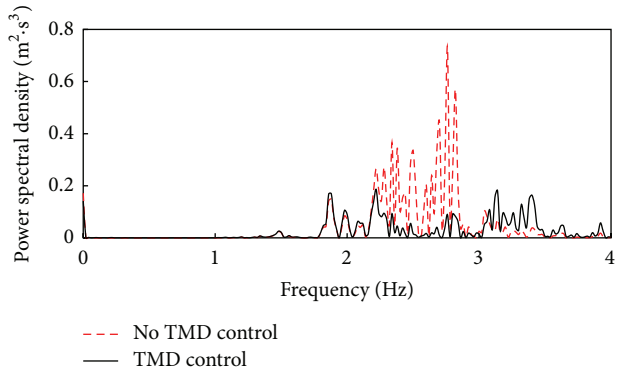

(a) Power spectral density of the acceleration under El-Centro NS seismic wave (TMD: tuned-mass damper)

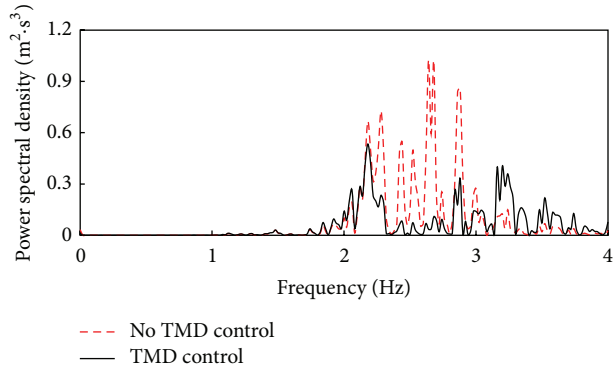

(b) Power spectral density of the acceleration under Taft EW seismic wave (TMD: tuned-mass damper)

Figure 9: Power spectral density of the acceleration under (a) the El-Centro NS and (b) the Taft EW seismic waves.

a numerical simulation and experimental investigation were provided about high response characteristics of the TMD and relative motion between the offshore platform and TMD.

5.1. High Response Characteristics. The duration of an earthquake excitation is generally short, and the maximum influence on a platform's deformation mainly results from its initial seconds. Therefore, it is critical that the high response speed of the TMD occurs within the initial seconds of the excitation. To overcome this problem, this study proposed a passive TMD without damper for improving the high response performance under critical earthquake loads.

By application of the central difference method, the displacements of the substructure and the main structure during the first 3 s of an excitation can be obtained. The initial conditions of main structure can be expressed as

$$\begin{aligned} x_1^{(0)} &= 0, \\ x_2^{(0)} &= 0, \\ x_1^{(1)} &= 0, \\ x_2^{(1)} &= 0. \end{aligned} \tag{12}$$

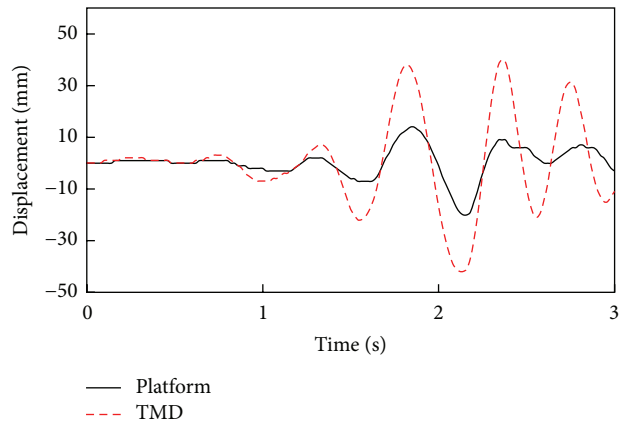

(a) Displacement responses under El-Centro NS seismic wave

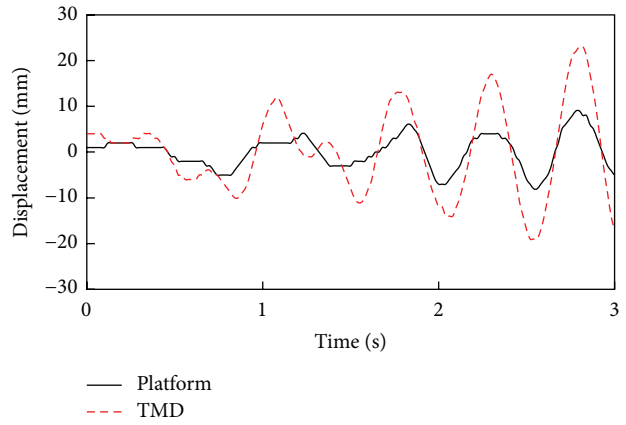

(b) Displacement responses under Taft EW seismic wave

FIGURE 10: Displacement responses of the tuned-mass damper (TMD) and platform under (a) the El-Centro NS and (b) the Taft EW seismic waves.

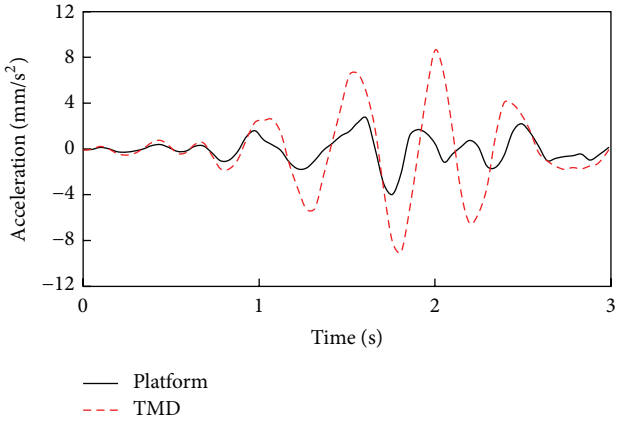

(a) Acceleration responses under El-Centro NS seismic wave

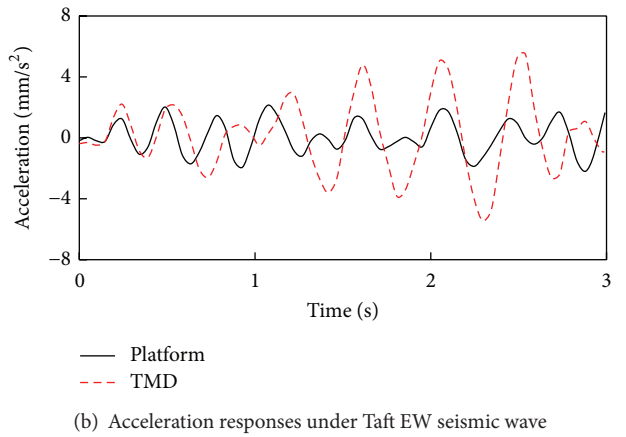

(b) Acceleration responses under Taft EW seismic wave

FIGURE 11: Acceleration responses of the tuned-mass damper (TMD) and platform under (a) the El-Centro NS and (b) the Taft EW seismic waves.

When the initial conditions of (12) are substituted into (6), the next-step differential displacements ${x_1}^{(2)}$ and ${x_2}^{(2)}$ can be obtained:

$$
\begin{aligned}
{x_1}^{(2)} &= \frac{-m_1 \ddot{x}_V \Delta^2 t}{m_1 + 0.5 c_1 \Delta t}, \\
{x_2}^{(2)} &= -\ddot{x}_V \Delta^2 t.
\end{aligned}
\tag{13}
$$

The ratio of ${x_1}^{(2)}$ and ${x_2}^{(2)}$ can be expressed as

$$
\frac{{x_1}^{(2)}}{{x_2}^{(2)}} = \frac{m_1}{m_1 + 0.5 c_1 \Delta t} < 1. \tag{14}
$$

It can be observed from (14), at the initial time, that the displacement of the substructure ${x_2}^{(2)}$ is always greater than the displacement of the main structure ${x_1}^{(2)}$; that is, ${x_2}^{(2)} > {x_1}^{(2)}$. Based on this theoretical analysis, an experiment was undertaken to investigate this high response phenomenon.

As illustrated in Figures 10 and 11, when the main structure begins to move under the earthquake excitation, the substructure also moves immediately. In addition, the displacement and acceleration of the substructure are both considerably greater than the main structure. This reveals that the substructure can achieve vibration suppression through its high response to the seismic excitations.

To understand the high response characteristics better, an FFT for the displacement responses was performed, and, then, the phase differences between the main structure and the substructure were calculated. The phase differences under the two seismic vibrations are presented in Figure 12. It can be observed that initial phase differences exist in different frequency domains, although they are only significantly high at frequencies other than around 1-2 Hz.

5.2. Relative Motion. In order to understand the dynamic performance more fully, it is necessary to study the relative motion between the main structure and the substructure. The model of the relative motion is shown in Figure 13, where x_1 and x_2 are the displacements of the main structure and the substructure, respectively. The motion between the main structure and the substructure can be divided into two parts: no relative motion ($|x_2 - x_1| = 0$) and relative motion ($|x_2 - x_1| \neq 0$), as illustrated in Figures 13(a) and 13(b),

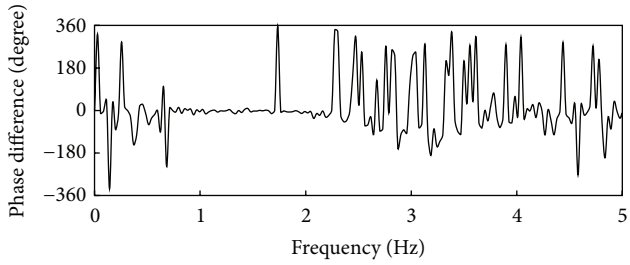

(a) Phase difference under El-Centro NS seismic wave

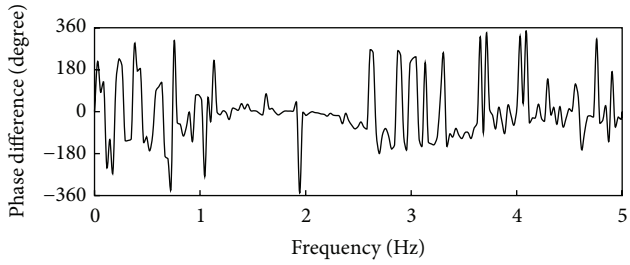

(b) Phase difference under Taft EW seismic wave

Figure 12: Phase differences of the tuned-mass damper (TMD) and platform under (a) the El-Centro NS and (b) the Taft EW seismic waves.

respectively. The elastic potential energy of the TMD can be written as

$$E_k = \frac{1}{2}k_2\left(x_2 - x_1\right)^2. \tag{15}$$

When $|x_2 - x_1| = 0$, the elastic potential energy becomes zero, which indicates that the total seismic vibrational energy is absorbed by the motion of the main structure. When $|x_2 - x_1| \neq 0$, part of the seismic vibrational energy is transferred to the elastic potential energy of the substructure. In this case, the relative motion can dissipate the partial seismic vibrational energy.

The relative displacements under the two seismic excitations are presented in Figure 14. It can be observed that intense relative motion exists throughout most of the time series. This type of intense relative motion produces elastic deformation of the spring, which can transfer part of the seismic energy to elastic potential energy.

5.3. Effectiveness Comparison. Up to now, there were few studies on the earthquake controlling for the jacket offshore platform; in particular, there are few researches concerning the high response performance of TMD system. Therefore, only two controllers of tuned-liquid damper [30] and an active mass damper [31], as the existing control schemes, were found for effectiveness comparison of the tuned-mass damper.

In Table 2, the reduction percentages are listed to compare their effectiveness about the peak oscillation amplitudes of the offshore platform. It can be observed that the reduction percentages of the tuned-mass damper, applied in this study, are relatively higher than that of the tuned-liquid damper and active mass damper. In fact, it is difficult to compare

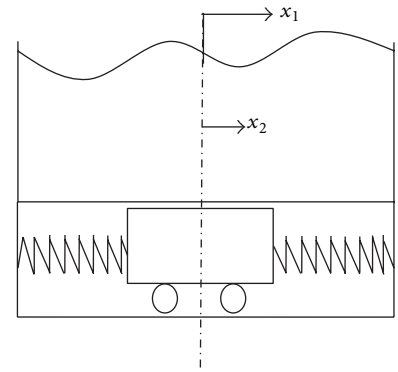

(a) $|x_2 - x_1| = 0$

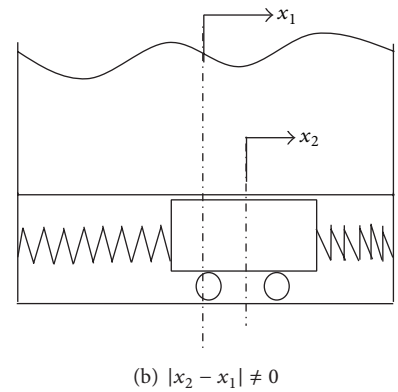

(b) $|x_2 - x_1| \neq 0$

Figure 13: Diagrams showing different relative motions: (a) no relative motion ($|x_2 - x_1| = 0$) and (b) relative motion ($|x_2 - x_1| \neq 0$).

Table 2: Effectiveness comparison of the control schemes.

Earthquake	Controllers	Reduction (%)	
		Displacement	Acceleration
El Centro	Tuned-liquid damper	17.6	11.28
	Active mass damper	16.7	−6.77
	Tuned-mass damper	28.05	32.39

them under a relatively fair condition due to their different experimental conditions. However, it is indicated that the high response characteristics can improve the earthquake controlling for the TMD control scheme in this study.

6. Conclusions

This study focused on vibration suppression of an offshore platform under earthquake loads by application of a TMD. The principles of the relevant mathematical modeling, tuning principle of the dynamic magnification factor, central difference method for numerical analysis, and evaluation indices were described, and an experimental system was constructed based on a 1 : 200-scale model of an actual four-column jack-up offshore platform. Specific experiments were performed for the offshore platform both with and without the TMD system under two types of seismic load. The effectiveness of the TMD system was investigated comprehensively by

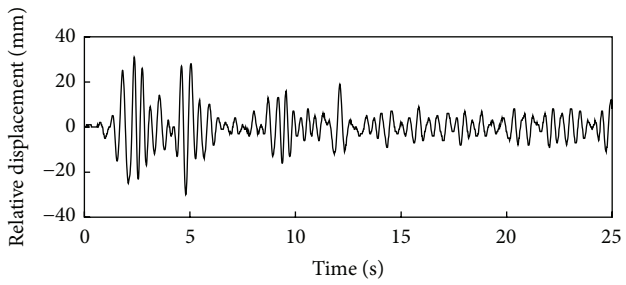

(a) Relative displacement under the El-Centro NS seismic wave

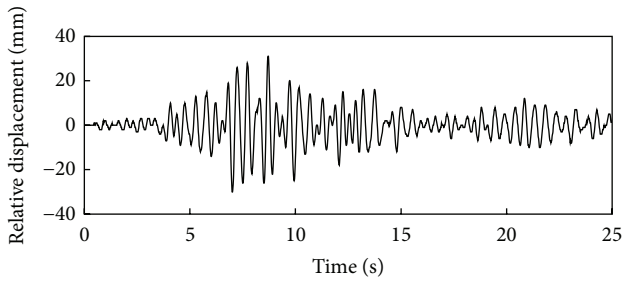

(b) Relative displacement under the Taft EW seismic wave

Figure 14: Relative displacements under (a) the El-Centro NS and (b) the Taft EW seismic waves.

analyses of the amplitude and frequency response, relative motion, high response characteristics, and evaluation indices.

Analyses of the amplitude and frequency responses indicated that the displacement, acceleration, and their power spectral density decreased significantly for the offshore platform with the TMD system. Further analyses of the high response and relative motion characteristics showed that the damping reaction started within the first 3 s of earthquake excitation, even only the fundamental nature frequency was consistently tuned for the TMD system. Consequently, the RMS ratios reached around 80% for the displacements and around 70% for the acceleration responses. The vibrating excitations of the offshore platform were improved significantly throughout the entire earthquake period. The relative ratio of the maximum peak values verified that a reduction of >27% was achieved for the maximum peak displacement response and a reduction of >32% was achieved for the acceleration response. Based on the numerical and experimental investigations of this study, it is verified that a passive TMD constitutes a simple but feasible measure for vibration suppression of offshore platforms exposed to earthquake excitations, mainly because of its high response characteristics.

Competing Interests

The authors declare that they have no competing interests.

Acknowledgments

The work described in this paper was supported by the Grant-in-Aid for Scientific Research (c) (Grant no. 24560271).

References

[1] J. Vazquez, R. Michel, J. Alford, M. Quah, and K. S. Foo, *Jack Up Units a Technical Primer for the Offshore Industry Professional*, Bennett & Associates, Offshore Technology Development, 2005.

[2] K. T. Chen, C. H. Chou, S. H. Chang, and Y. H. Liu, "Intelligent active vibration control in an isolation platform," *Applied Acoustics*, vol. 69, no. 11, pp. 1063–1084, 2008.

[3] H. Yu, X. Li, and S. Yang, "Dynamic analysis method of offshore jack-up platforms in regular and random waves," *Journal of Marine Science and Application*, vol. 11, no. 1, pp. 111–118, 2012.

[4] R. J. Hunt and P. D. Marsh, "Opportunities to improve the operational and technical management of jack-up deployments," *Marine Structures*, vol. 17, no. 3-4, pp. 261–273, 2004.

[5] M. S. Williams, R. S. G. Thompson, and G. T. Houlsby, "Nonlinear dynamic analysis of offshore jack-up units," *Computers and Structures*, vol. 69, no. 2, pp. 171–180, 1998.

[6] M. J. Terro, M. S. Mahmoud, and M. A. Rohman, "Multi-loop feedback control of offshore steel jacket platforms," *Computers and Structures*, vol. 70, no. 2, pp. 185–202, 1999.

[7] G. W. Housner, L. A. Bergman, T. K. Caughey et al., "Structural control: past, present, and future," *Journal of Engineering Mechanics*, vol. 123, no. 9, pp. 897–971, 1997.

[8] B. Zhang and Q. Han, "Network-based modelling and active control for offshore steel jacket platform with TMD mechanisms," *Journal of Sound and Vibration*, vol. 333, no. 25, pp. 6796–6814, 2014.

[9] H. H. Lee, S. Wong, and R. Lee, "Response mitigation on the offshore floating platform system with tuned liquid column damper," *Ocean Engineering*, vol. 33, no. 8-9, pp. 1118–1142, 2006.

[10] B. Zhang, L. Ma, and Q. Han, "Sliding mode H_∞ control for offshore steel jacket platforms subject to nonlinear self-excited wave force and external disturbance," *Nonlinear Analysis. Real World Applications*, vol. 14, no. 1, pp. 163–178, 2013.

[11] B. Zhang, Q. Han, and X. Zhang, "Event-triggered H_∞ reliable control for offshore structures in network environments," *Journal of Sound and Vibration*, vol. 368, no. 25, pp. 1–21, 2016.

[12] B. Zhang, Q. Han, X. Zhang, and X. Yu, "Sliding mode control with mixed current and delayed states for offshore steel jacket platforms," *IEEE Transactions on Control Systems Technology*, vol. 22, no. 5, pp. 1769–1783, 2014.

[13] V. Gattulli and R. Ghanem, "Adaptive control of flow-induced oscillations including vortex effects," *International Journal of Non-Linear Mechanics*, vol. 34, no. 5, pp. 853–868, 1999.

[14] K. Kawano, "Active control effects on dynamic response of offshore structures," in *Proceedings of the 3rd International Offshore and Polar Engineering Conference*, pp. 594–598, June 1993.

[15] Y. Zhou, L. Xu, and Z. Li, "Seismic response of semi-active control using magneto-rheological fluid dampers," *Journal of Civil Engineering*, vol. 34, no. 5, pp. 10–14, 2001.

[16] J. Ou, X. Long, Q. S. Li, and Y. Q. Xiao, "Vibration control of steel jacket offshore platform structures with damping isolation systems," *Engineering Structures*, vol. 29, no. 7, pp. 1525–1538, 2007.

[17] J. L. Almazán, J. C. De la Llera, J. A. Inaudi, D. López-García, and L. E. Izquierdo, "A bidirectional and homogeneous tuned mass damper: a new device for passive control of vibrations," *Engineering Structures*, vol. 29, no. 7, pp. 1548–1560, 2007.

[18] S. Chakraborty and B. K. Roy, "Reliability based optimum design of Tuned Mass Damper in seismic vibration control of structures with bounded uncertain parameters," *Probabilistic Engineering Mechanics*, vol. 26, no. 2, pp. 215–221, 2011.

[19] M. Domizio, D. Ambrosini, and O. Curadelli, "Performance of tuned mass damper against structural collapse due to near fault earthquakes," *Journal of Sound and Vibration*, vol. 336, pp. 32–45, 2015.

[20] C. Li and B. Zhu, "Estimating double tuned mass dampers for structures under ground acceleration using a novel optimum criterion," *Journal of Sound and Vibration*, vol. 298, no. 1-2, pp. 280–297, 2006.

[21] G. Bekdaş and S. M. Nigdeli, "Estimating optimum parameters of tuned mass dampers using harmony search," *Engineering Structures*, vol. 33, no. 9, pp. 2716–2723, 2011.

[22] H. Yu, F. Gillot, and M. Ichchou, "Reliability based robust design optimization for tuned mass damper in passive vibration control of deterministic/uncertain structures," *Journal of Sound and Vibration*, vol. 332, no. 9, pp. 2222–2238, 2013.

[23] T. Pinkaew, P. Lukkunaprasit, and P. Chatupote, "Seismic effectiveness of tuned mass dampers for damage reduction of structures," *Engineering Structures*, vol. 25, no. 1, pp. 39–46, 2003.

[24] A. Ghosh and B. Basu, "Effect of soil interaction on the performance of tuned mass dampers for seismic applications," *Journal of Sound and Vibration*, vol. 274, no. 3–5, pp. 1079–1090, 2004.

[25] C. Lin, J. Ueng, and T. Huang, "Seismic response reduction of irregular buildings using passive tuned mass dampers," *Engineering Structures*, vol. 22, no. 5, pp. 513–524, 2000.

[26] H. Tsai, "The effect of tuned-mass dampers on the seismic response of base-isolated structures," *International Journal of Solids and Structures*, vol. 32, no. 8-9, pp. 1195–1210, 1995.

[27] C. Lin, L. Lu, G. Lin, and T. Yang, "Vibration control of seismic structures using semi-active friction multiple tuned mass dampers," *Engineering Structures*, vol. 32, no. 10, pp. 3404–3417, 2010.

[28] Z. Zhang and T. Balendra, "Passive control of bilinear hysteretic structures by tuned mass damper for narrow band seismic motions," *Engineering Structures*, vol. 54, pp. 103–111, 2013.

[29] G. C. Marano, R. Greco, F. Trentadue, and B. Chiaia, "Constrained reliability-based optimization of linear tuned mass dampers for seismic control," *International Journal of Solids and Structures*, vol. 44, no. 22-23, pp. 7370–7388, 2007.

[30] Q. Jin, X. Li, N. Sun, J. Zhou, and J. Guan, "Experimental and numerical study on tuned liquid dampers for controlling earthquake response of jacket offshore platform," *Marine Structures*, vol. 20, no. 4, pp. 238–254, 2007.

[31] J. P. Ou, X. Long, Q. S. Li, and Y. Q. Xiao, "Experimental research on AMD control of structural vibration of offshore platform," *High Technology Letters*, no. 10, pp. 85–90, 2002 (Chinese).

[32] D. Xie, *Introduction to Offshore Platform Design*, Huazhong University of Technology, 2008.

[33] K. Seto, *Dynamic Vibration Absorber and Its Application*, CORONA Publishing, 2010.

[34] S. S. Rao, *Mechanical Vibration*, Prentice Hall, 5th edition, 2010.

[35] National Research Institute for Earth Science and Disaster Prevention, January 2015, http://www.kyoshin.bosai.go.jp/kyoshin/quake/.

[36] I. Takewaki, A. Moustafa, and K. Fujita, *Improving the Earthquake Resilience of Buildings: The Worst Case Approach*, Springer Series in Reliability Engineering, 2013.